Polymer Chemistry

Cite this: *Polym. Chem.*, 2012, **3**, 2057

www.rsc.org/polymers

PAPER

Synthesis, self-assembly and stimuli responsive properties of cholesterol conjugated polymers

Sema Sevimli,[a] Sharon Sagnella,[a] Maria Kavallaris,[ac] Volga Bulmus[b] and Thomas P. Davis*[a]

Received 29th February 2012, Accepted 11th April 2012
DOI: 10.1039/c2py20112g

Reversible addition–fragmentation chain transfer (RAFT) polymerization was used to generate well-defined pH-responsive biofunctional polymers as potential 'smart' gene delivery systems. A series of five poly(dimethylamino ethyl methacrylate-*co*-cholesteryl methacrylate) P(DMAEMA-*co*-CMA) statistical copolymers, with similar molecular weights and varying cholesterol content, were prepared. The syntheses, compositions and molecular weight distributions for P(DMAEMA-*co*-CMA) were monitored by nuclear magnetic resonance (NMR), solid-state NMR and gel permeation chromatography (GPC) evidencing well-defined polymeric structures with narrow polydispersities. Aqueous solution properties of the copolymers were investigated using turbidimetry and light scattering to determine hydrodynamic diameters and zeta potentials associated with the phase transition behaviour of P(DMAEMA-*co*-CMA) copolymers. UV-Visible spectroscopy was used to investigate the pH-responsive behaviour of copolymers. Hydrodynamic radii were measured in the range 10–30 nm (pH, temperature dependent) by dynamic light scattering (DLS). Charge studies indicated that P(DMAEMA-*co*-CMA) polymers have an overall cationic charge, mediated by pH. Potentiometric studies revealed that the buffering capacity and pK_a values of polymers were dependent on cholesterol content as well as on cationic charge. The buffering capacity increased with increasing charge ratio, overall demonstrating transitions in the pH endosomal region for all five copolymeric structures. Cell viability assay showed that the copolymers displayed increasing cytotoxicity with decreasing number of cholesterol moieties. These preliminary results show the potential of these well-defined P(DMAEMA-*co*-CMA) polymers as *in vitro* siRNA delivery agents.

Introduction

Gene therapy research is a rapidly progressing field with vast potential for the treatment of a variety of diseases including muscular dystrophies, influenza, arthritis, osteoporosis, Alzheimer's disease, asthma, cancer and AIDS.[1–3] Small interfering RNAs (siRNA), *double-stranded products of 21–23 nucleotides*,[4] are vital agents in the RNA interference (RNAi) process, which is aimed to specifically suppress a gene expression by breaking down the target mRNA.[5] siRNA has emerged as a promising therapeutic strategy due to its target specific gene silencing mechanism; however, its low *in vivo* stability and poor cellular uptake hinder its therapeutic effect.[6] To overcome these drawbacks non-viral transfection vectors such as cationic polymers have been developed to protect an siRNA and enhance its intracellular delivery. Polycationic nonviral gene carriers benefit from greater flexibility, improved safety, and facile manufacturing,[7,8] as they offer advanced therapeutic efficacy with doses of siRNA that are substantially lower and/or delivered less frequently than otherwise.[9] Synthetic cationic polymers which have been used in gene transfection include poly(ethylenimine) (PEI),[10] poly(amidoamine) (PAMAM) dendrimer,[11] poly(histidine),[12] poly(L-lysine),[12,13] and chitosan.[14] Specific physicochemical characteristics, such as chemical structure, pK_a values, molecular weight and molecular weight distribution, water solubility and architecture, must be taken into account upon optimizing the transfection efficiency of cationic polymers.[15] ExGen 500®, a linear PEI, has been developed as a transfection reagent with a high transfection efficiency.[16] In comparison to branched PEI (25 kD), linear PEI (22 kD) has exhibited superior proton sponge properties by inducing membrane destabilization and facilitating the endosomal escape of gene polyplexes.[17,18] Consequently cationic polymers that are able to protonate over a wider range of pH, similar to linear PEI (22 kD), may display efficient gene delivery properties. 2-(Dimethylamino) ethyl methacrylate (DMAEMA), a tertiary amine with low pK_a, was chosen as the cationic component in our copolymer structure. DMAEMA has been recognized for its

[a]*Australian Centre for Nanomedicine (ACN), The University of New South Wales, Sydney, NSW 2052, Australia. E-mail: t.davis@unsw.edu.au*
[b]*Department of Chemical Engineering, Izmir Institute of Technology, Gulbahce, İzmir, 35430, Turkey*
[c]*Children's Cancer Institute Australia (CCIA), Lowy Cancer Research Centre, The University of New South Wales, Sydney, NSW 2052, Australia*

ability to complex and protect nucleotides while facilitating endosomal escape through the proton sponge mechanism.[19,20] Although cationic groups are primarily responsible for gene binding and endosomal escape, when systemically administered these positively charged complexes induce cytotoxicity. One strategy to lower the cytotoxicity and enhance the stability of polyplexes is to incorporate hydrophobic moieties.[21]

The enhancement of cell-membrane transport of therapeutics can be achieved by using small hydrophobic and/or bulky lipid groups, such as cholesterol, that can interact with cell membranes.[22] Cholesterol is an essential structural component of the plasma membrane, which is distributed heterogeneously, where it typically accounts for 20–25% of the lipid molecules.[23] Cholesterol participates in forming semipermeable barriers between cellular compartments, regulates membrane fluidity,[23] modulates the function of various membrane proteins,[24,25] and takes part in several membrane trafficking and trans-membrane signaling processes.[26] Cholesterol conjugation to an siRNA has been described by others to enhance the cytoplasmic delivery of an siRNA while eliciting RNA interference (RNAi), resulting in specific gene silencing.[27,28] Due to the proven effect of cholesterol on the transport of therapeutics across the cell-membrane, we have developed well-defined cholesterol containing, pH-responsive, cationic polymers *via* reversible addition–fragmentation chain transfer (RAFT) polymerization as potential carriers in siRNA delivery applications.

RAFT is a living radical polymerization process invented by CSIRO.[29] As a synthetic technique, RAFT offers a convenient platform for molecular engineering of polymeric systems for drug delivery, biotechnology, nanotechnology and nanomedicine applications.[30–37] It has already been used to synthesise a range of polymeric structures for siRNA delivery,[38–46] with certain RAFT generated polymers found to have low levels of cytotoxicity.[47,48]

In this study a novel polycationic system that is capable of self-assembly in aqueous solutions and of forming small, stable nanoparticles when complexed to siRNAs has been synthesized, imbuing nonviral carrier characteristics such as gene protection, phase transition and buffering capacity. A series of well-defined P(DMAEMA-*co*-CMA) copolymers, with varying amounts of CMA, were made and characterized.

Experimental section

Materials

Cholesterol (Sigma, 98%), methacryloyl chloride (Fluka, >97%), dichloromethane (Univar, analytical grade reagent), tetrahydrofuran (THF) (Univar, analytical grade reagent), toluene (Univar, analytical grade reagent), dioxane (Univar, analytical grade reagent), citric acid (Univar), methanol (Univar, analytical grade reagent), acetone (Univar, analytical grade reagent), ethanol (Univar, analytical grade reagent), sodium phosphate monobasic (Univar), phosphate buffer saline (PBS) pellets (Sigma), sodium phosphate dibasic (Univar), Roswell Park Memorial Institute (RPMI) (Gibco, Invitrogen), Dulbecco's Modified Eagle Medium (DMEM) (Gibco, Invitrogen), 10% Fetal Calf Serum (FCS) were used as received. High purity nitrogen (Linde gases, 99.99%) was used for purging the reaction solutions before polymerization. 2-(Dimethylamino) ethyl methacrylate (DMAEMA) monomer (Aldrich, 98%) was purified *via* basic alumina gel column chromatography before use. The initiator, 2,2-azobisisobutyronitrile (AIBN), was recrystallized twice from methanol prior to use. Triethylamine (Sigma-Aldrich, 99%) was stored with sodium hydroxide pellets (Univar) for 2 days prior to use. 4-(Cyanopentanoic acid)-4-dithiobenzoate (CPADB), used as a RAFT agent, was synthesized according to the procedure described in the literature.[49,50] AlamarBlue dye was prepared by mixing 75 mg resazurin sodium salt (Sigma), 12.5 mg methylene blue hydrate (Sigma), 164.5 mg potassium hexacyanoferrate(III) (Sigma) and 211 mg potassium hexacyanoferrate(II) trihydrate (Sigma) in 500 mL of sterile PBS. Membranes for dialysis (MWCO 3500) were purchased from Fisher Biotech (Cellu SepT4, regenerated cellulose-Tubular membrane).

Analytical techniques

Nuclear magnetic resonance (NMR) spectroscopy. ^{1}H NMR spectra were measured using a Bruker DPX 300 MHz spectrometer, while ^{13}C NMR spectra were measured using a Bruker Avance III 400 MHz NMR Spectrometer. $CDCl_3$ was used as the solvent for solution state NMR analyses.

Solid-state nuclear magnetic resonance spectroscopy. The ^{13}C solid-state NMR spectra were recorded on a Bruker Avance III 300 MHz solid-state NMR spectrometer equipped with a 4 mm standard bore cross-polarization magic angle spinning (CPMAS) probe head. 100 mg of each polymer sample was packed down into 4 mm MAS rotors, and analysed with the cross-polarization procedure (CP) under magic angle spinning (MAS). ^{13}C spectra were recorded at a spinning frequency of 12 kHz.

Gel permeation chromatography (GPC). Gel permeation chromatography was performed using HPLC grade dimethylacetamide (DMAc) as the mobile phase. Polymer solutions (3–5 mg mL^{-1} in DMAc) were injected into GPC at 40 °C (flow rate = 1 mL min^{-1}). A Shimadzu modular system comprising an SIL-10AD auto-injector, a PL 5.0 mm bead-size guard column (50 × 7.8 mm) followed by four linear PL (Styragel) columns (10^5, 10^4, 10^3, and 100 Å) was used. Calibration was achieved with commercial polystyrene standards ranging from 500 to 10^6 g mol^{-1}.

Attenuated total reflection-Fourier transform infrared (ATR-FTIR) spectroscopy. ATR-FTIR measurement was carried out with a Bruker IFS66/S High End FT-NIR/IR Spectrometer system using diffuse reflectance sampling accessories and a resolution of 4 cm^{-1}. The monomer sample was analyzed using 256 scans.

Methods

Cholesteryl methacrylate monomer synthesis. Cholesteryl methacrylate (CMA) monomer was synthesized according to a modified procedure in contradistinction to the literature.[51,52] In brief, cholesterol (2.0 g, 0.02 mol) was dissolved in the mixture of toluene containing triethylamine (5 mL, 23% v/v triethylamine/toluene) in a 100 mL round bottom flask with a stirrer bar. The solution was left under reflux for 1 hour at 60 °C. Methacryloyl

chloride (3.3 mL, 0.60 mol) along with the remaining triethylamine–toluene mixture (11.25 mL, 23% v/v triethylamine/toluene) was added drop wise over a period of 30 minutes and the solution was refluxed for an additional 12 hours. After the solution reached room temperature the product, cholesteryl methacrylate (CMA), was purified by precipitating in 1.6 N HCl–methanol from toluene. The white colored precipitate, CMA, was dried under vacuo overnight generating a yield of 88% (Fig. 1).

^{1}H NMR ($CDCl_3$, δ in ppm): 6.1, 5.5 (m, 2H, CH_2=C(CH_3)COO-), 5.3 (d, 1H, J = 4.9 Hz, -C=CH-, olefin group in cholesterol), 4.6 (m, 1H, -COO-CH-), 1.9 (s, 3H, -CH_2=C(CH_3)COO-), 0.93 (d, 3H, J = 6.6 Hz, -CH-CH_3), 0.88, 0.84 (d, 3H, J = 4.8 Hz, -CH-(CH_3)$_2$), 0.68 (s, 3H, -C-CH_3).

Solid-state ^{13}C NMR (δ in ppm): 162.5 (-COO-), 137.5 (-C=CH-, olefin group in cholesterol), 134.7 (-CH_2=C(CH_3)COO-), 121.4 (-CH_2=C(CH_3)COO-), 119.2 (-C=CH-, olefin group in cholesterol), 71.1 (-COO-CH-), 16.1 (-CH_2=C(CH_3)COO-).

ATR-FTIR (cm^{-1}): 3100–2700 (alkene and alkane C–H stretching), 1716 (C=O stretching), 1639 (C=C stretching), 1160 (C–O–C stretching) (Fig. 2).

CMA monomer has been quantified in the literature with a molar mass of 454 g mol^{-1} (ref. 52) which has been confirmed with the following elemental analysis: C%, 81.87; H%, 11.09; O%, 7.04.[53]

Synthesis of poly(dimethylamino ethyl methacrylate). The syntheses of poly(dimethylamino ethyl methacrylate)

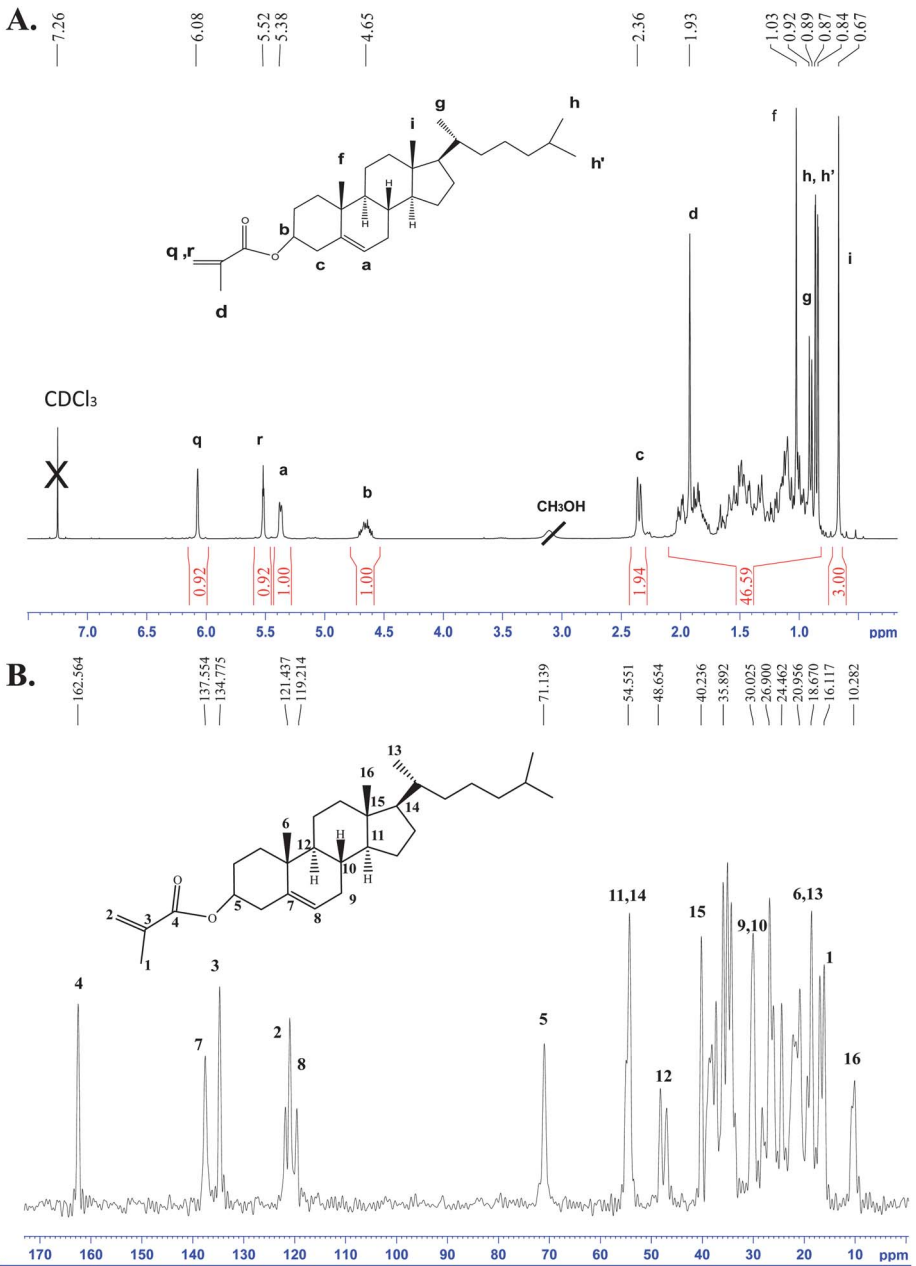

Fig. 1 (A) ^{1}H NMR spectra of cholesteryl methacrylate monomer in $CDCl_3$ solvent using a Bruker 300 MHz NMR spectrometer, at 298 K; (B) ^{13}C solid-state NMR spectra on a Bruker Avance III 300 MHz solid-state NMR spectrometer.

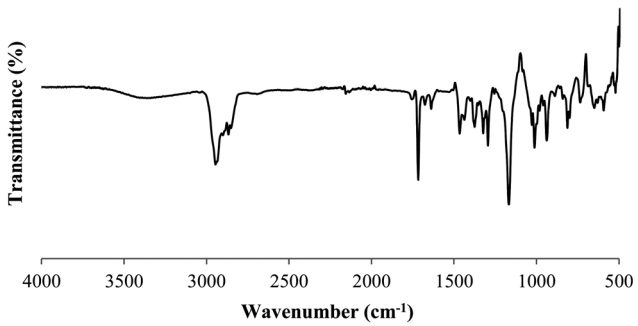

Fig. 2 FT-IR spectra of cholesteryl methacrylate monomer.

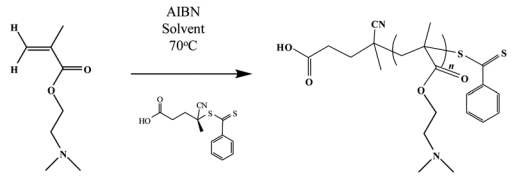

Scheme 1 Synthesis of P(DMAEMA) *via* RAFT polymerization.

(PDMAEMA) (Scheme 1) were performed using varying feed ratios and experimental conditions (Table 1). Briefly, DMAEMA monomer (500 mg, 3.2 mmol), RAFT agent, 4-(cyanopentanoic acid)-4-dithiobenzoate (CPADB), and initiator, 2,2-azobisisobutyronitrile (AIBN), were dissolved in toluene and sealed in flasks. The solutions were purged with N_2 (g) for 20 minutes in an ice bath. The solutions were then placed in an oil bath at 70 °C. The monomer conversions were determined by ^{1}H NMR analyses of the crude polymerization mixtures (Fig. 3).

^{1}H NMR ($CDCl_3$, δ in ppm): 4.08 (t, 2H, $J = 11$ Hz, -COO-CH_2-CH_2-), 2.57 (t, 2H, $J = 11$ Hz, -COO-CH_2-CH_2-), 2.30 (s, 6H, -N-$(CH_3)_2$), 1.86 (s, 2H, CH_2-C-), 0.98 (s, 3H, -C-CH_3).

The comparative molecular weights of the polymers were obtained by GPC using DMAc as the mobile phase.

RAFT copolymerization of dimethylamino ethyl methacrylate and cholesteryl methacrylate. Statistical copolymerizations of the monomers were conducted (experimental details are shown in Table 2). DMAEMA and CMA monomers, CPADB, and AIBN were dissolved in toluene. The solutions were sealed in vials with rubber septa and then degassed using nitrogen for 30 minutes in an ice bath. The polymerizations were carried out at temperatures of 68 °C. The monomer conversions were determined by ^{1}H NMR analyses of the crude polymerization mixtures (Fig. 6).

^{1}H NMR ($CDCl_3$, δ in ppm): 5.38 (d, 1H, $J = 4.9$ Hz, -C=CH-, olefin group in cholesterol), 4.51(m, 1H, -COO-CH-), 4.08 (t, 2H, $J = 11$ Hz, -COO-CH_2-CH_2-), 2.57 (t, 2H, $J = 12.2$ Hz, -COO-CH_2-CH_2-), 2.30 (s, 6H, -N-$(CH_3)_2$), 1.86 (s, 2H, CH_2-C-), 0.98 (s, 3H, -C-CH_3), 0.93 (d, 3H, $J = 6.6$ Hz, -CH-CH_3), 0.88–0.84 (d, 3H, $J = 4.8$ Hz, -CH-$(CH_3)_2$), 0.68 (s, 3H, -C-CH_3).

The comparative molecular weights of the polymers were obtained by GPC using DMAc as the mobile phase. Copolymers were purified by a two-step process; initially P(DMAEMA-*co*-CMA) was dialyzed against a 98% ethanol–water mixture for 4 days. Samples were subjected to rotary evaporation (to remove ethanol) and then freeze-dried (to remove water). Finally the copolymers were dissolved in acidic aqueous solution (10 mM HCl solution prepared with deionized water) and transferred to dialysis tubing (MWCO: 3500). The solutions were dialyzed against deionized water for 3 days followed by freeze-drying, giving a light-pink powder. The final pure copolymers were analysed by solid-state ^{13}C NMR (Fig. 7).

Solid-state ^{13}C NMR (δ in ppm): 162.5 (-COO-), 137.5 (-C=CH-, olefin group in cholesterol), 119.2 (-C=CH-, olefin group in cholesterol), 71.1 (-COO-CH-), 59.7 (-COO-CH_2-CH_2-), 56.3 (-COO-CH_2-CH_2-), 43.8 (-N-$(CH_3)_2$), 16.1 (-CH_2=$C(CH_3)$COO-).

Characterization of basicity and protonation. The buffering capacity of P(DMAEMA-*co*-CMA) copolymers was investigated *via* acid–base titrations using combined protocols described elsewhere.[15,54,55] Each polymer was made into an aqueous solution (20 mL) at concentrations of 0.2 mg mL^{-1}. Under continuous stirring, solutions were first titrated with 0.1 M NaOH until the pH value reached 11, and then back-titrated with 0.1 M HCl. The pH was measured using a Metrohm Ion Analysis 827 pH lab meter from MEPinstruments. All measurements were carried out in duplicate at 25 °C. Finally 'pH *vs.* volume$_{HCl}$' plots were generated to characterize the pH profile of each copolymer.

Optical density measurements. UV-Visible spectroscopy was used to analyze the pH-responsive phase behaviors of polymers by measuring the turbidity change of polymer solutions at varying pH values.[56] Citric-phosphate buffer solutions (0.1 M) ranging from pH 3.0 to pH 7.4 were prepared. The ionic strengths of the buffer solutions were adjusted to 0.1 M by the addition of NaCl to yield isotonic solutions. Six different polymer samples, P(DMAEMA-*co*-CMA) (0% CMA, cholesterol mole content of 0% with number average molecular weight

Table 1 Experimental conditions for polymerization of DMAEMA

[DMAEMA]/[RAFT]/[AIBN][a]	Solvent	Time (h)	Conversion[b] (%)	M_n[c] (g mol^{-1})	PDI[d]	$M_{n,theo}$[e]
164.0/1.0/0.10	Dioxane	24	66	15 270	1.17	17 000
200.0/1.0/0.20	Dixoane	8	57	17 230	1.17	17 900
252.0/1.0/0.22	Dioxane	10	75	21 600	1.21	28 500
252.0/1.0/0.22	Toluene	10	81	25 500	1.19	31 800
200.0/1.0/0.20	THF	8	68	n/a	n/a	21 300

[a] Polymerization conditions, temperature 70 °C. [b] Monomer conversion determined by ^{1}H NMR. [c] The number average molecular weight determined by DMAc GPC analysis using PS standards. [d] Polydispersity index. [e] The theoretical molecular weight calculated by $M_{n,theo} = ([M]_o/[RAFT]_o) \times$ conversion $\times$ $MW_{monomer}$, where $[M]_o$, $[RAFT]_o$, conversion, $MW_{monomer}$ are the initial monomer and RAFT agent concentrations, monomer conversion and molecular weight of the monomer respectively.

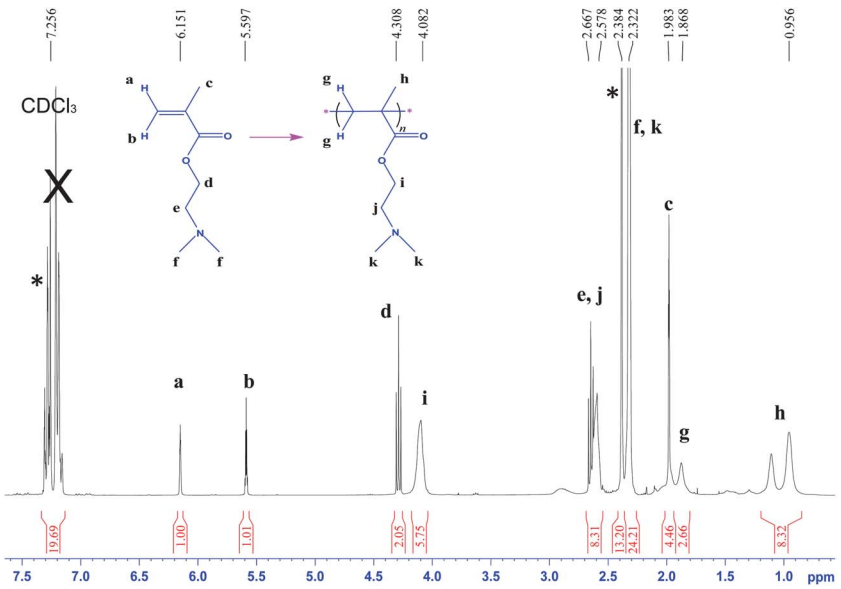

Fig. 3 ^{1}H NMR spectra of PDMAEMA in $CDCl_3$ using a Bruker 300 MHz NMR spectrometer, at 298 K. Polymerization conditions were 8.3 M : 0.033 M : 7.16 mM [DMAEMA] : [RAFT] : [AIBN] at 70 °C in toluene for 10 hours. Polymer conversions were calculated according to the equation given as follows: $[(\int i/2)/((\int i/2) + (\int d/2))] \times 100\%$. Solvent peaks are represented with the asterisk symbol (*).

$(M_n)_{GPC}$ of 26 800 g mol^{-1}; 2% CMA, cholesterol mole content of 2% with $(M_n)_{GPC}$ 21 900 g mol^{-1}; 4% CMA, cholesterol mole content of 4% with $(M_n)_{GPC}$ 23 500 g mol^{-1}; 8% CMA, cholesterol mole content of 8% with $(M_n)_{GPC}$ 21 800 g mol^{-1}; 15% CMA, cholesterol mole content of 15% with $(M_n)_{GPC}$ 23 500 g mol^{-1}; 20% CMA, cholesterol mole content of 20% with $(M_n)_{GPC}$ 20 400 g mol^{-1}) were dissolved in buffer solutions at 0.128 μmol mL^{-1} concentration. The absorbance of each polymer solution from acidic pH to neutral pH was detected by a double beam UV-Vis Spectrophotometer (Hitachi, U-2800) using UV solutions 2.1 software. Polymer solutions were measured at 400 nm using quartz cuvettes. Assays were repeated three times.

Dynamic light scattering (DLS). Dynamic light scattering studies were performed using a Malvern Instruments Zetasizer Nano ZS Instrument (Malvern, USA) equipped with a 4 mV He–Ne laser operating at $\lambda = 633$ nm, an avalanche photodiode detector with high quantum efficiency, and an ALV/LSE-5003 multiple tau digital correlator electronics system. The polymer sample solutions were prepared with appropriate buffers at 3 mg mL^{-1} concentration. All samples were measured by scanning 7 times with each time of automatic measurement. Assays were done in triplicate.

ζ-Potential measurements. ζ-Potential measurements were performed using a Malvern Instruments Zetasizer NaNo ZS Instrument (Malvern, USA) equipped with a 4 mV He–Ne laser operating at $\lambda = 633$ nm, an avalanche photodiode detector with high quantum efficiency, and an ALV/LSE-5003 multiple tau digital correlator electronics system. The polymer sample solutions were prepared with neutral and acidic buffers at 3 mg mL^{-1} concentration. Readings were taken in Folded Capillary cells DTS1060 (Malvern Instruments) and recorded in millivolts (mV). All measurements were done in triplicate.

Determination of cell viability *via* AlamarBlue assay. Human lung cancer (H460) cells and normal human foetal lung fibroblasts (MRC5) were used to assess polymer toxicity. H460 cells were grown in Roswell Park Memorial Institute (RPMI) medium with HEPES and L-glutamine, while MRC5 cells were grown in Dulbecco's Modified Eagle Medium (DMEM) containing 4.5 g L^{-1} glucose and L-glutamine; both mediums were supplemented with 10% Fetal Calf Serum (FCS). For the cell viability assay,

Table 2 Data of copolymers prepared at varying compositions

$[M]_t$[a]	[DMAEMA]/[CMA]/[RAFT]/[AIBN]	CMA in feed (mol% of total monomer)	Polymer composition (CMA mole ratio)	Conversion[b] (%)	M_n[c] (g mol^{-1})	PDI[d]
4.15	247.0/5.03/1.00/0.22	2	2	73	21 900	1.14
4.15	238.7/12.5/1.00/0.22	4	4	93	23 500	1.18
4.15	231.8/20.1/1.00/0.22	8	8	86	21 800	1.12
4.15	214.3/37.7/1.00/0.22	15	15	94	23 500	1.12
4.15	202.0/50.3/1.00/0.22	20	20	89	20 400	1.19

[a] Total monomer concentration, polymerization conditions, solvent toluene and temperature 68 °C. [b] Monomer conversion determined by ^{1}H NMR. [c] The number of average molecular weight determined by DMAc GPC analysis using PS standards. [d] Polydispersity index.

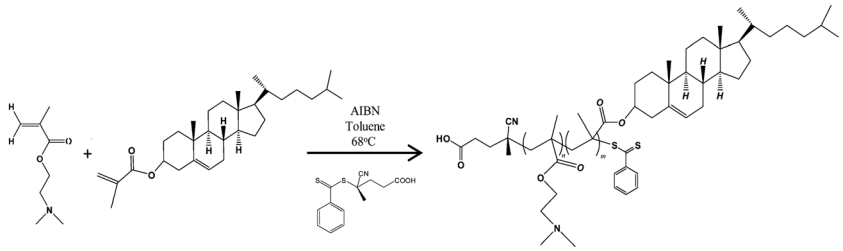

Scheme 2 Synthesis of P(DMAEMA-*co*-CMA) *via* RAFT polymerization.

H460 and MRC5 cells were seeded in 96-well plates at final concentrations of 2.5×10^3 cells mL^{-1} and 5×10^3 cells mL^{-1}, respectively, and grown at 37 °C in 5% CO_2 and 95% humidity for 24 hours to ensure adherence. Upon surface attachment cells were treated with polymer solutions at varying concentrations from 0.005 μM to 50 μM and were further incubated for 72 hours. After the incubation period, 20 μL of AlamarBlue was added to each well, and incubated for another 6 hours. Absorbance was measured by a Benchmark Plus Microplate Spectrophotometer (Bio-Rad Laboratories) that uses the MPM-III software program at 570 nm_{Ex}/595 nm_{Em}. The percentage of viability was calculated by comparing treated cells with positive control cells representing 100% viability:

$$\% \text{ Cell viability} = [(A_P - A_B)/(A_C - A_B)] \times 100$$

A_P and A_C are the absorbances of cells treated with polymer solutions (at varying concentrations) and control cells (cells only in media, positive control for 100% viability) respectively. A_B is the absorbance of blank wells (wells with media and polymer treatment, no cells) where the values are similar to 10% Triton X-100 treatment which corresponds to 0% viability. The treatments were done with 5 replicates; overall the assay was repeated three times using cells at different passage numbers.

Results and discussion

Cholesteryl methacrylate monomer synthesis

Cholesteryl methacrylate (**CMA**) was synthesized at high yields and purity. Complete NMR characterization of this product was performed by solution state ^1H NMR and ^{13}C NMR along with solid-state ^{13}C NMR spectra confirming the expected product.

Synthesis of poly(dimethylamino ethyl methacrylate)

Before performing copolymerizations of **CMA** with DMAEMA, homopolymerizations of each monomer were studied under the same conditions. To determine the optimal reaction conditions to synthesize P(DMAEMA), different feed mole ratios of [DMAEMA]/[RAFT]/[AIBN] were examined (Table 1). THF, toluene and dioxane were the solvents selected to facilitate polymerization of CMA and DMAEMA monomers in a homogeneous phase. Polymer conversions in dioxane were lower than those in the corresponding toluene experiments. Solvent effects on free radical polymerization reactions are notoriously difficult to attribute to elementary events;[57] suffice to say that dioxane is an electron-donor solvent, with the potential to interact with the electron-acceptor carbonyl group of DMAEMA.[58]

According to the results, 252.0/1.0/0.22 ([DMAEMA]/[RAFT]/[AIBN]) in toluene had the highest conversion. This ratio with an overall feed concentration of 8.3 M : 0.033 M : 7.16 mM ([DMAEMA] : [RAFT] : [AIBN]) produced a polymer with 25 500 g mol^{-1} molecular weight and a PDI of 1.19. Throughout further investigations the feed concentration was halved to 4.15 M : 0.017 M : 3.58 mM ([DMAEMA] : [RAFT] : [AIBN]) intending to lower the $(M_n)_{GPC}$ and PDI whilst optimising the chain end integrity of the polymer.

RAFT copolymerization and kinetic studies

Enhancement of cytoplasmic delivery of macromolecular therapeutics can be achieved by using lipid structures, such as cholesterol – an important component of cell membranes,[59] that promote membrane tethering and endocytosis into endosomes by interacting with the cell membrane.[22] We hypothesized that by incorporating cholesterol units into pH-sensitive synthetic polymers, the cell-membrane activity of cholesterol could be tuned in a pH-dependent manner.

We thus used the RAFT technique to generate potential siRNA carriers from well-defined pH-responsive, statistical copolymers of **DMAEMA** with differing ratios of **CMA**, esterified cholesterol. P(DMAEMA-*co*-CMA) was prepared *via* RAFT polymerization, using **CPABD**, a dithioester RAFT agent widely used amongst methacrylate polymerizations,[60] and AIBN as an initiator (Scheme 2).

Polymerizations were performed in toluene using 4.15 M as the total monomer concentration, at a feed ratio of 4.07 M : 0.08 M : 0.017 M : 3.58 mM [DMAEMA] : [CMA] : [RAFT] : [AIBN]

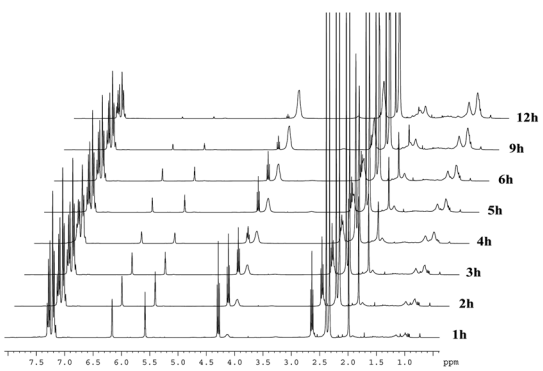

Fig. 4 ^1H NMR spectra of P(DMAEMA-*co*-CMA) in $CDCl_3$ solvent using a Bruker 300 MHz NMR spectrometer, at 298 K. 2% CMA feed composition. Polymerization conditions 4.07 M : 0.08 M : 0.017 M : 3.58 mM [DMAEMA] : [CMA] : [RAFT] : [AIBN] at 68 °C in toluene at predetermined time points (1 h, 2 h, 3 h, 4 h, 5 h, 6 h, 9 h, 12 h).

at 68 °C, yielding a number average molecular weight $(M_n)_{GPC}$ of 21 900 g mol^{-1} (polydispersity index (PDI) = 1.14) at a monomer conversion of ~73%. The experimental molecular weight determined by GPC was close to the theoretical value (*i.e.*, 21 900–30 000 g mol^{-1}) calculated by the equation $M_{n,theo}$ = ([M]$_o$/[RAFT]$_o$) × conversion × $MW_{monomer}$, where [M]$_o$, [RAFT]$_o$, conversion, $MW_{monomer}$ are the initial monomer and RAFT agent concentrations, monomer conversion and molecular weight of the monomer respectively.

The polymerization kinetics of P(DMAEMA-*co*-CMA) (4.07 M : 0.08 M : 0.017 M : 3.58 mM [DMAEMA] : [CMA] : [RAFT] : [AIBN]) in toluene were monitored by ^{1}H NMR at varying time points (1 h, 2 h, 3 h, 4 h, 5 h, 6 h, 9 h, 12 h) (Fig. 4). The overlayed ^{1}H NMR spectra depict the vinylic protons of both CMA and DMAEMA decreasing with increasing time, indicative of the expected result for a successful polymerization.

Fig. 5A displays the GPC traces of P(DMAEMA-*co*-CMA) (obtained at [DMAEMA]/[CMA]/[RAFT]/[AIBN] = 247.0/5.03/1.00/0.22) suggesting the occurrence of a monomodal molecular weight distribution during polymerization in toluene. It is evident from GPC traces that the molecular weight of the P(DMAEMA-*co*-CMA) increases with polymerization time. Fig. 5B reveals a semi-logarithmic monomer conversion (determined by ^{1}H NMR) implying that monomer conversion increases concomitantly with time. The advancement of M_n with monomer conversion (Fig. 5C) exhibits a linear pseudo-first order kinetic behavior with a narrow polydispersity profile for the produced polymers. Consequently,

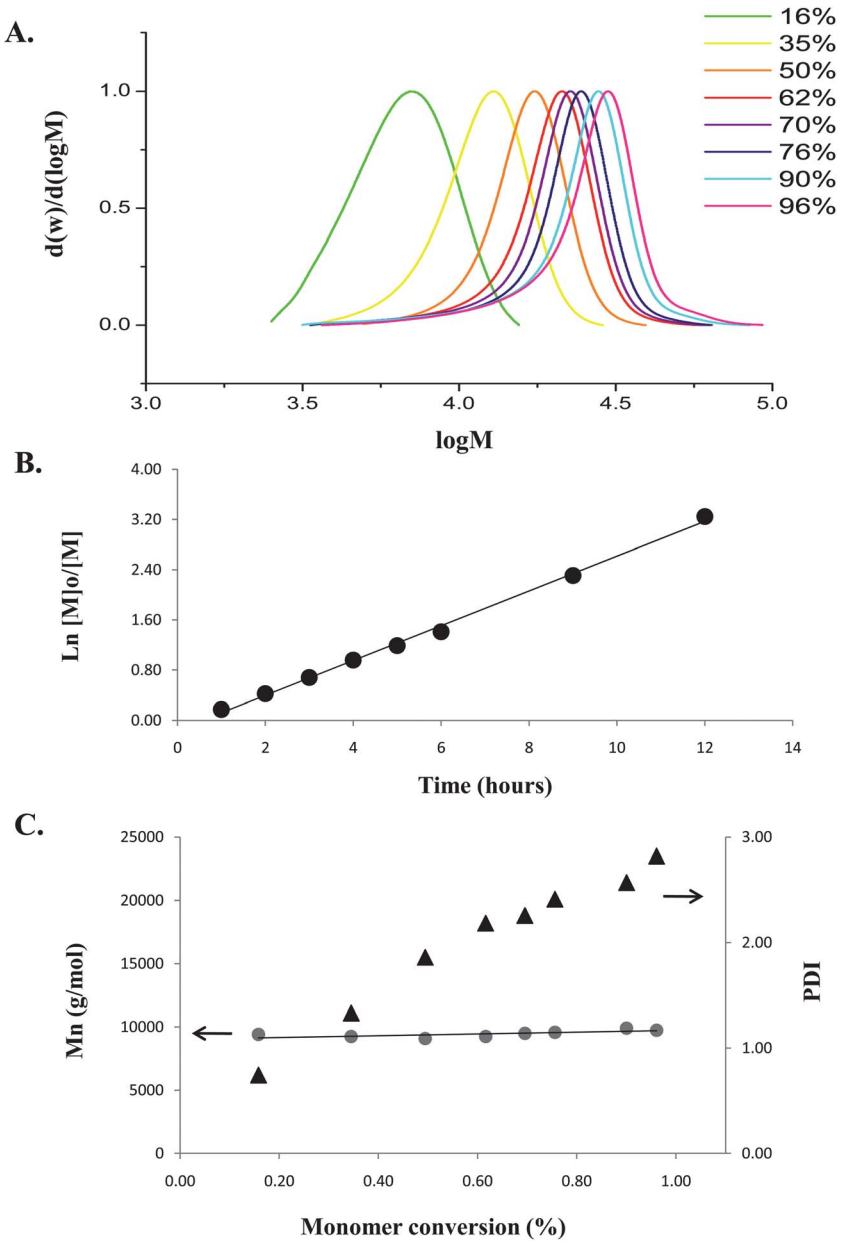

Fig. 5 Results from RAFT polymerizations of P(DMAEMA-*co*-CMA) in toluene at 68 °C ([DMAEMA]/[CMA]/[RAFT]/[AIBN] = 247.0/5.03/1.00/0.22). (A) GPC traces of P(DMAEMA-*co*-CMA) synthesized at different polymerization times (from DMAc GPC); (B) Ln[M]$_o$/[M] *vs.* time; and (C) Number average molecular weight $(M_n)_{GPC}$ (triangles) and PDI (circles) *vs.* monomer conversion.

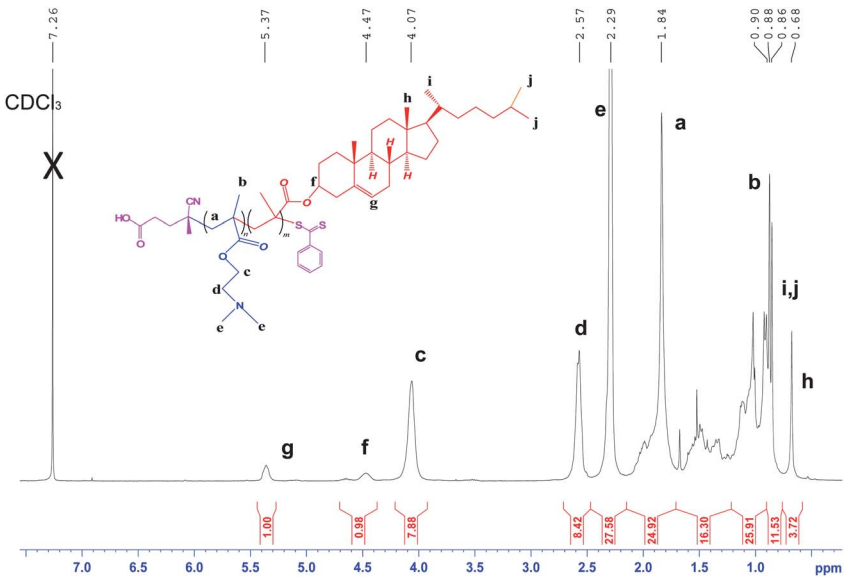

Fig. 6 ^{1}H NMR of purified P(DMAEMA-*co*-CMA) (M_n determined by GPC, 23 500 g mol^{-1}; and PDI 1.12) in $CDCl_3$, obtained after dialysis against 98% ethanol–water mixture. Polymerization conditions 3.52 M : 0.622 M : 0.017 M : 3.58 mM [DMAEMA] : [CMA] : [RAFT] : [AIBN] at 68 °C in toluene for 9 hours. Copolymer compositions were determined by the ^{1}H NMR spectrum resulting in CMA units: 20% mol; DMAEMA units: 80% mol. Copolymer composition was calculated according to the equation given as follows: CMA mol% $= \left[\int f/(\int c/2) + (\int f)\right] \times 100\%$; DMAEMA mol% $= \left[(\int c/2)/(\int c/2) + (\int f)\right] \times 100\%$.

both narrow molecular weight distributions and the linear increase of molecular weights with monomer conversion indicate that the RAFT polymerization of P(DMAEMA-*co*-CMA) displayed the known traits of living radical polymerization.[61]

Purified polymers were analyzed by ^{1}H NMR using $CDCl_3$ as the solvent (Fig. 6). Peaks at 5.3 and 4.5 ppm, indicative of olefinic hydrogen in the cholesterol moiety and methine, –COO–*CH*–, the main link between the cholesterol moiety and ester group, were observed in equal intensities, suggesting good polymerization with cholesterol units intact. Polymerization was proven to be very efficient with the disappearance of signals at 6.15 and 5.60 ppm (ethylene group –*H*–) along with those at 6.10 and 5.56 ppm (olefin peaks), characteristic peaks of DMAEMA and CMA respectively.

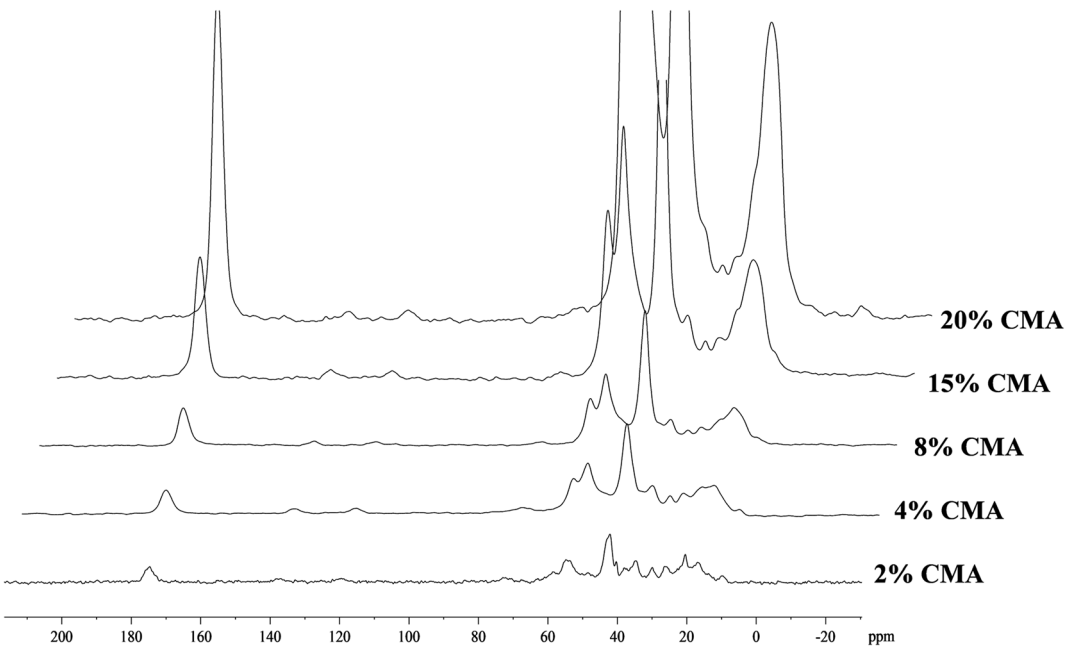

Fig. 7 Solid-state ^{13}C NMR of purified P(DMAEMA-*co*-CMA) (copolymer compositions 2% CMA, 4% CMA, 8% CMA, 15% CMA, 20% CMA) obtained after reversible quarternization. Polymerization conditions 4.15 M : 0.017 M : 3.58 mM [total monomer] : [RAFT] : [AIBN] at 68 °C in toluene for 9 hours.

After confirming that DMAEMA and CMA can be readily copolymerized under typical RAFT conditions, amphiphilic statistical copolymers with increasing hydrophobic units were prepared and further analyzed. A library of 8 statistical copolymers was synthesized with CMA mol% of 2%, 4%, 8%, 15%, 20%, 30%, 40% and 50%. The amphiphilic character of copolymers decreased with increasing cholesterol content making reversible quarternization necessary to obtain particles in aqueous solution. In accord with previous findings,[62] copolymers prepared with 20% CMA or less exhibited complete water solubility and were chosen for further physicochemical analysis (Table 2).

With the intention of confirming the molecular structure and water solubility of quarternized copolymers, ^{1}H NMR spectra were examined in the presence of D_2O. However, structure visualization was hindered by D_2O interfering with the sensitivity and spectral resolutions of olefinic cholesterol peaks. As an alternative technique, solid-state ^{13}C NMR spectroscopy, a powerful tool used for the investigation of various materials such as polymers and, for the last decade, biomolecules,[63] was used for the characterization of copolymers, with evidential success. The solid-state ^{13}C NMR spectra portray efficient polymerization with the disappearance of peaks at 134.7 ppm and 121.4 ppm (CMA monomer signals) together with those at 136.0 ppm and 125.2 ppm (characteristic DMAEMA monomer peaks) confirming the ^{1}H NMR spectra. The spectrum allows polymer compositions to be validated through integration ratios between cholesterol peaks at 137.5 ppm and 119.2 ppm which intensify with increasing CMA units (Fig. 7).

Characterization of basicity and protonation

Buffering capacity is defined as the percentage of amine groups becoming protonated over an 11 to 2 pH range. The buffering capacity of potential gene carriers is a significant factor since the property will have a direct impact on the ability to effectively condense, protect and deliver genes.[55,64] The presence of amine units in our copolymers was expected to make them more protonable over a broad pH range. Consequently, P(DMAEMA-*co*-CMA) copolymers with varying cholesterol content were examined by acid–base titrations. The profiles of titration curves with hydrochloric acid (HCl) clearly revealed that copolymers carrying more amine groups displayed a wider buffering capacity (Fig. 8). Copolymers with 2% CMA showed the strongest buffering ability, whereas copolymers with 20% CMA showed the least buffering capacity.

Table 3 Buffering range and effective pK_a values of statistical copolymers of P(DMAEMA-*co*-CMA)

Polymer	Tertiary amine content (%)	Buffering range	Effective pK_a value
2% CMA	98	8.50–4.59	5.91
4% CMA	96	7.79–4.39	5.79
8% CMA	92	7.64–4.19	5.65
15% CMA	85	7.32–4.42	5.45
20% CMA	80	7.11–4.23	5.39

Effective pK_a values were calculated from the inflection points of these titration curves (Table 3).[65] The pK_a values varied between 5.39 and 5.91 which is less than pK_a 7.4 (550 kD)–7.8 (4 kD) of PDMAEMA or of DMAEMA monomer (pK_a 8.4).[66,67] The shift to acidic pK_a can be explained by the cholesterol units contributing to an increase in the overall hydrophobicity. Investigations suggest copolymers with greater hydrophobicity manifest reduced dielectric constants influencing the deprotonation of amine groups, therefore displaying lower pK_a values.[68] Results indicate that 2% CMA (lowest cholesterol units) in comparison to 20% CMA (highest cholesterol units) exhibits a higher pK_a value, which is in agreement with previous reports.[15,69]

Acid–base titrations show that the buffering capacity for statistical P(DMAEMA-*co*-CMA) copolymers decreases with increasing CMA content; their effective pK_a values (5.39–5.91) allow them to potentially protonate and become strong polycations in the endosomal pH making them excellent candidates to facilitate endosomal escape by the "proton sponge effect".[20,70–72]

Aqueous solution properties

Polymer chains equipped with ionisable units and hydrophobic groups hold interesting pH-responsive properties when dissolved in aqueous media.[73] The pH-induced phase transitions of P(DMAEMA-*co*-CMA) copolymers, in aqueous solutions, were investigated by turbidity, light scattering and ζ-potential measurements.

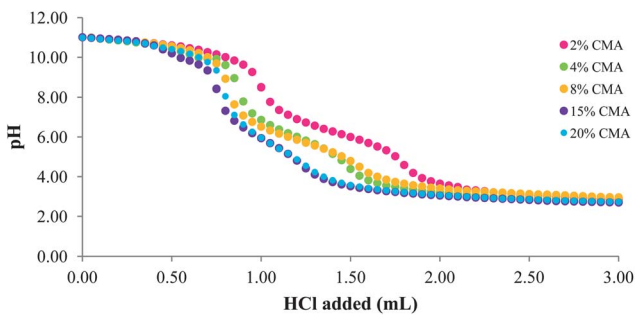

Fig. 8 Potentiometric titration curves for statistical copolymers of 2% CMA, 4% CMA, 8% CMA, 15% CMA and 20% CMA representing 2%, 4%, 8%, 15%, 20% mole ratio of CMA in P(DMAEMA-*co*-CMA) respectively.

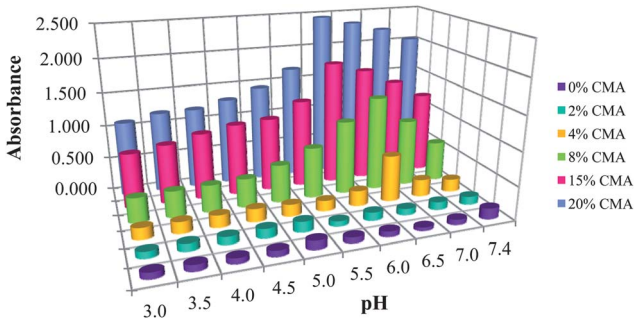

Fig. 9 Absorbance values at 400 nm of P(DMAEMA-*co*-CMA) polymers prepared with 0% CMA, 2% CMA, 4% CMA, 8% CMA, 15% CMA and 20% CMA mole ratios, from acidic to neutral pH solutions at 0.125 μmol mL^{-1}.

Optical density measurements. The turbidity profiles of P(DMAEMA-*co*-CMA) copolymers, prepared with varying CMA units, were observed in a range of pH 3.0–12.0. The pH-dependent absorbance for the aqueous solutions of P(DMAEMA-*co*-CMA) at 0.128 μmol mL^{-1} (~3 mg mL^{-1}) were measured at 400 nm by UV-Vis spectrometry. In Fig. 9, the turbidity changes of polymer solutions with increasing hydrophobic units are shown from acidic to neutral pH. Polymers carrying 0% CMA and 2% CMA retained transparent solutions throughout the pH changes, evidencing the absence of large scatter formation despite their pK_a values. At increased molar ratios of CMA, P(DMAEMA-*co*-CMA) demonstrated significant elevation of absorbance at all values of pH. The competitive interactions between electrostatic repulsion and hydrophobic interactions seen in P(DMAEMA-*co*-CMA) play a crucial role in determining the pH-dependent phase transition of polymers in aqueous solution.[73] Under neutral conditions molecules seem to be relatively compact due to their hydrophobic groups causing turbidity in solution. Upon protonation of the amino groups in acidic pH, electrostatic repulsive forces take effect, expanding the polymer chain, increasing its solubility and resulting in enhanced solvation. Irregular absorbance patterns were displayed under basic conditions suggesting the formation of unstable aggregates (data not included).[74]

The pH-responsive turbidity profiles of P(DMAEMA-*co*-CMA) copolymers are illustrated in two regions; the transparent range where pH < pK_a and the turbid range at pH ≈ pK_a or pH > pK_a. Fig. 9 reveals a drastic increase in absorbance for polymer solutions between pH 4.5 and 6.5. This is attributed to both the hydrophobic units arising from CMA and the enhanced hydrophobic effect emanating from the deprotonation of amine groups. The effective pK_a's calculated from potentiometric titration experiments revealed that increased hydrophobicity (CMA mol% ratio) lowered the pK_a values (2% CMA = 5.91, 4% CMA = 5.79, 8% CMA = 5.65, 15% CMA = 5.45 and 20% CMA = 5.39). As a result, P(DMAEMA-*co*-CMA) with the highest hydrophobic ratio, 20% CMA, had the lowest p*K*a 5.39, subsequently demonstrating a phase transition at the lowest pH region (pH ≈ 5.0). Accordingly, with decreasing hydrophobic components (<20% CMA) the pH region for phase transition exhibited higher values (5.0 < pH < 6.0).

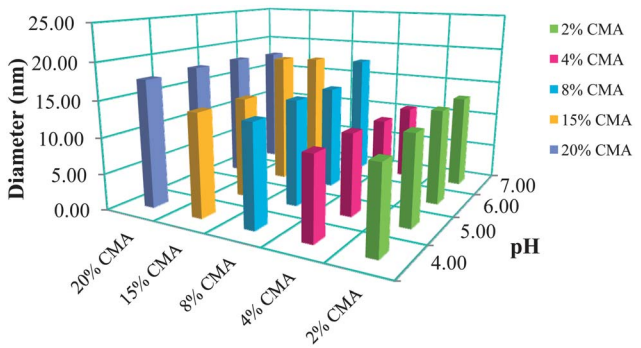

Fig. 10 DLS results for copolymers with 2% CMA, 4% CMA, 8% CMA, 15% CMA and 20% at different pH values (25 °C). Anova statistical error values show the results to be within * $P < 0.005$ accuracy.

Dynamic light scattering and zeta-potential measurements. The pH-induced aqueous solution behaviour of P(DMAEMA-*co*-CMA) copolymers was further studied *via* DLS and zeta-potential measurements. The effective diameter of each copolymer in solution was investigated over the range pH 4.0 to pH 10.0 at both 25 °C and 37 °C. It is evident from Fig. 10 that at low pH values (pH < pK_a) amine groups on DMAEMA protonate, as indicated by transparent polymer solutions, with consistent hydrodynamic radii. Upon shifting to higher pH (>8.0), amine units begin to deprotonate and thus form unstable aggregates.[66,73,74] The effective diameter displayed by polymers in aqueous solutions increased from 11 nm to 18 nm as the amount of CMA increased from 2 to 20 mol%. In agreement with previous research, particle size increases proportionally with the hydrophobic (bulky) content in the copolymers (copolymers containing 20% CMA exhibited the largest hydrodynamic diameter).[75] Increasing temperature had a slight effect by enlarging their hydrodynamic radii (data not shown).

To determine the effective surface charge of P(DMAEMA-*co*-CMA) copolymers, the zeta potential was measured at 2 different pH values (pH 5.0 and 7.4) at 25 °C as shown in Fig. 11, and at 37 °C as shown in Table 4.

The zeta potentials of the copolymers increased from +27 mV to +36 mV at pH 7.4 (25 °C) and approached +47 mV from +38 mV at pH 5.0 (25 °C) when the feed molar ratio of CMA units decreased from 20% to 0%. This result is in accord with higher charge densities in copolymers with less CMA (as expected). At lower pH values, below the pK_a point, the amine groups of DMAEMA become protonated and increased the overall charge density.[76] Potentially, this protonation property of the copolymers will help escape the acidified endosomes exploiting the "proton sponge effect".[77]

Cytotoxicity assay. The cytotoxicity profiles of P(DMAEMA-*co*-CMA), prepared with varying CMA units, were evaluated by an AlamarBlue Cell Viability Assay on both human lung cancer (H460) cells and normal human foetal lung (MRC5) cells. AlamarBlue, an established cell viability indicator,[78] benefits from the reduction reactions that take place in metabolically active cells where resazurin (nontoxic, non-fluorescent indicator dye) is converted to resorufin, a bright red fluorescent molecule.[79] Fig. 12 displays the viability of H460 and MRC5 cells after 72 hours as a function of polymer treatments at varying concentrations (0.005–50 μM).

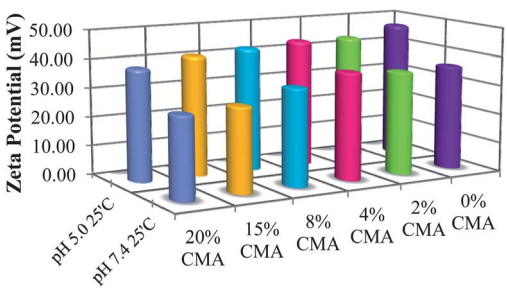

Fig. 11 ζ-Potential measurements of copolymers containing 0% CMA, 2% CMA, 4% CMA, 8% CMA, 15% CMA and 20% CMA under acidic and neutral conditions (25 °C). Anova statistical error values show the results to be within * $P < 0.0005$ accuracy.

Table 4 ζ-Potential values for copolymers under acidic and neutral conditions at 37 °C

Zeta potential (mV)						
37 °C	20% CMA	15% CMA	8% CMA	4% CMA	2% CMA	0% CMA
pH 5.0	22.07	21.27	38.83	40.27	40.63	38.43
pH 7.4	21.27	20.17	32.13	35.60	36.87	36.10

For both carcinoma and healthy cell lines at concentrations below 5 μM P(DMAEMA-*co*-CMA) copolymers displayed no toxicity, demonstrating comparable cytotoxicity results with cationic polymers like poly-L-lysine (PLL),[80] poly(ethylenimine) (PEI),[21] poly(amidoamine) (PAMAM),[80] and PDMAEMA. Cationic polymers have received great attention, as they can readily form stable nanostructures with nucleic acids and mediate transfection with high efficacy whilst eluding difficulties triggered by the use of viral vectors for gene delivery.[81] However, these molecules exhibit high cytotoxicity due to their cationic nature. Some methods used to reduce toxicity have been (not limited too) masking the charges and/or incorporating hydrophobic moieties.[82] Taking this into consideration, P(DMAEMA-*co*-CMA) copolymers have demonstrated lower toxicity (at higher concentrations (5 μM)) with CMA units increased up to 15% and 20% (Fig. 12A). Copolymers with 2%, 4%, and 8% CMA mole units displayed IC_{50} values of 1.5, 1.6, and 1.8 μM, respectively, which are higher than those reported for the 'gold standard' references PEI ((25 000 g mol^{-1}) (0.2–0.8 μM))[21,83] and commercially available jetPEI (0.3 to 1.3 μM)[84] in various cell lines (HeLa, 4TI, MDAMB435). It should be stressed that a maximum increase in cell viability (H460 cell line) was achieved with copolymers of 15% and 20% CMA demonstrating (IC_{50} values of 5.0 and 21 μM respectively) the positive effect CMA moieties had on polymer toxicity. The concentrations of copolymers necessary for *in vitro* gene transfection studies are expected to be lower than their IC_{50} values. The results potentially make P(DMAEMA-*co*-CMA) useful cationic candidates for future transfection studies.

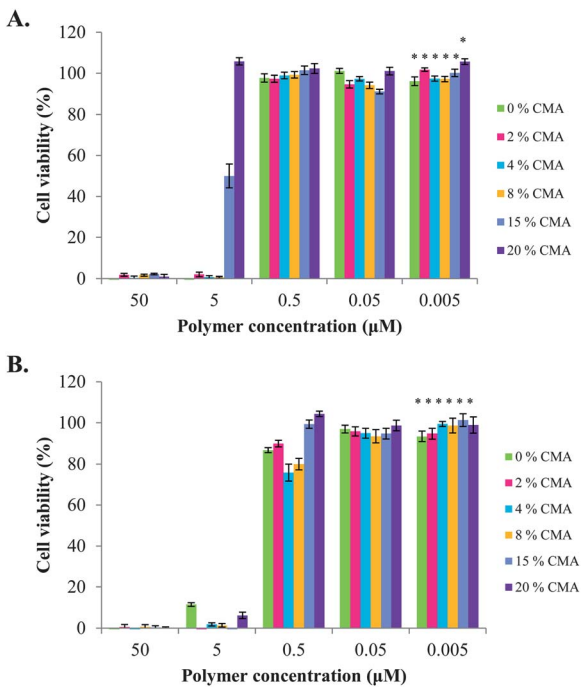

Fig. 12 Viability of (A) human lung cancer H460 cells and (B) normal human foetal lung (MRC5) cells after incubation with P(DMAEMA-*co*-CMA) copolymers that consist of 2%, 4%, 8%, 15% and 20% CMA along with P(DMAEMA) (0% CMA) for 72 hours, measured with AlamarBlue assay. The assay was repeated three times in 5 replicates and the viability results were normalized according to the positive control (untreated cells). Error bars represent standard deviation. Anova statistical error values show the results to be within * $P < 0.005$ accuracy.

Conclusion

In conclusion, a series of pH-responsive biosynthetic amphiphilic copolymers of P(DMAEMA-*co*-CMA), with varying cholesterol units, were synthesized *via* RAFT polymerization. The effect of hydrophobic units on copolymer composition, self-assembly in aqueous solutions and physicochemical properties was investigated. Kinetics studies revealed well-defined polymeric structures with narrow molecular weight distributions, indicating a living RAFT polymerization. The copolymer compositions influenced pK_a values and consequently copolymer buffering capacity. The amphiphilic copolymers showed pH-induced phase transitions in aqueous media originating from protonation of the amine groups as verified by turbidity, light scattering and zeta-potential measurements. Cell viability assays revealed that the copolymers displayed decreasing toxicity with increasing number of cholesterol moieties.

The characterization of P(DMAEMA-*co*-CMA) copolymers, reported herein, suggests that they are excellent candidates as potential drug and gene carriers for pharmaceutical applications. Future work will focus on *in vitro* studies on P(DMAEMA-*co*-CMA) copolymers and will evaluate the copolymer utility for condensing and transporting siRNA.

Acknowledgements

We gratefully acknowledge The University of New South Wales Analytical Centre NMR Facilities, with special thanks to Dr James Hook and Dr Rasmus Linser, for their expertise and technical assistance. We acknowledge Professor Les Field (DVCR UNSW) and Professor Graham Davies (Dean of Engineering, UNSW) for substantial strategic funding to establish the Australian Centre for Nanomedicine.

References

1 J. H. Jeong, S. W. Kim and T. G. Park, *Prog. Polym. Sci.*, 2007, **32**, 1239–1274.
2 D. Castanotto and J. J. Rossi, *Nature*, 2009, **457**, 426–433.
3 K. Tiemann and J. J. Rossi, *EMBO Mol. Med.*, 2009, **1**, 142–151.
4 A. Kwok and S. L. Hart, *Nanomed.: Nanotechnol., Biol. Med.*, 2011, **7**, 210–219.

5 J. Jeong, T. Park and S. Kim, *Pharm. Res.*, 2011, **28**, 2072–2085.
6 Y.-W. Won, S.-M. Yoon, K.-M. Lee and Y.-H. Kim, *Mol. Ther.*, 2011, **19**, 372–380.
7 D. W. Pack, A. S. Hoffman, S. Pun and P. S. Stayton, *Nat. Rev. Drug Discovery*, 2005, **4**, 581–593.
8 S. Lin, F. S. Du, Y. Wang, S. P. Ji, D. H. Liang, L. Yu and Z. C. Li, *Biomacromolecules*, 2008, **9**, 109–115.
9 D. Bumcrot, M. Manoharan, V. Koteliansky and D. W. Y. Sah, *Nat. Chem. Biol.*, 2006, **2**, 711–719.
10 A. Richards Grayson, A. Doody and D. Putnam, *Pharm. Res.*, 2006, **23**, 1868–1876.
11 A. P. Perez, E. L. Romero and M. J. Morilla, *Int. J. Pharm.*, 2009, **380**, 189–200.
12 Q. Leng, P. Scaria, J. Zhu, N. Ambulos, P. Campbell and A. J. Mixson, *J. Gene Med.*, 2005, **7**, 977–986.
13 T. Segura and J. A. Hubbell, *Bioconjugate Chem.*, 2007, **18**, 736–745.
14 K. A. Howard, S. R. Paludan, M. A. Behlke, F. Besenbacher, B. Deleuran and J. Kjems, *Mol. Ther.*, 2008, **17**, 162–168.
15 L. Veron, A. Ganee, M. T. Charreyre, C. Pichot and T. Delair, *Macromol. Biosci.*, 2004, **4**, 431–444.
16 A. von Harpe, H. Petersen, Y. Li and T. Kissel, *J. Controlled Release*, 2000, **69**, 309–322.
17 J. P. Behr, *Chimia*, 1997, **51**, 34–36.
18 C. L. Gebhart and A. V. Kabanov, *J. Controlled Release*, 2001, **73**, 401–416.
19 P. van de Wetering, N. M. E. Schuurmans-Nieuwenbroek, W. E. Hennink and G. Storm, *J. Gene Med.*, 1999, **1**, 156–165.
20 C. H. Zhu, S. Jung, G. Y. Si, R. Cheng, F. H. Meng, X. L. Zhu, T. G. Park and Z. Y. Zhong, *J. Polym. Sci., Part A: Polym. Chem.*, 2010, **48**, 2869–2877.
21 Y. Wang, L. S. Wang, S. H. Goh and Y. Y. Yang, *Biomacromolecules*, 2007, **8**, 1028–1037.
22 V. Incani, A. Lavasanifar and H. Uludag, *Soft Matter*, 2010, **6**, 2124–2138.
23 E. Ikonen, *Nat. Rev. Mol. Cell Biol.*, 2008, **9**, 125–138.
24 G. Gimpl and K. Gehrig-Burger, *Steroids*, 2011, **76**, 216–231.
25 T. J. Pucadyil and A. Chattopadhyay, *Prog. Lipid Res.*, 2006, **45**, 295–333.
26 V. Cherezov, D. M. Rosenbaum, M. A. Hanson, S. G. F. Rasmussen, F. S. Thian, T. S. Kobilka, H.-J. Choi, P. Kuhn, W. I. Weis, B. K. Kobilka and R. C. Stevens, *Science*, 2007, **318**, 1258–1265.
27 C. Wolfrum, S. Shi, K. N. Jayaprakash, M. Jayaraman, G. Wang, R. K. Pandey, K. G. Rajeev, T. Nakayama, K. Charrise, E. M. Ndungo, T. Zimmermann, V. Koteliansky, M. Manoharan and M. Stoffel, *Nat. Biotechnol.*, 2007, **25**, 1149–1157.
28 J. Soutschek, A. Akinc, B. Bramlage, K. Charisse, R. Constien, M. Donoghue, S. Elbashir, A. Geick, P. Hadwiger, J. Harborth, M. John, V. Kesavan, G. Lavine, R. K. Pandey, T. Racie, K. G. Rajeev, I. Rohl, I. Toudjarska, G. Wang, S. Wuschko, D. Bumcrot, V. Koteliansky, S. Limmer, M. Manoharan and H.-P. Vornlocher, *Nature*, 2004, **432**, 173–178.
29 G. Moad, E. Rizzardo and S. H. Thang, *Aust. J. Chem.*, 2005, **58**, 379–410.
30 C. Boyer, V. Bulmus, T. P. Davis, V. Ladmiral, J. Q. Liu and S. Perrier, *Chem. Rev.*, 2009, **109**, 5402–5436.
31 H. T. T. Duong, C. P. Marquis, M. Whittaker, T. P. Davis and C. Boyer, *Macromolecules*, 2011, **44**, 8008–8019.
32 C. Boyer, M. H. Stenzel and T. P. Davis, *J. Polym. Sci., Part A: Polym. Chem.*, 2011, **49**, 551–595.
33 Z. F. Jia, L. J. Wong, T. P. Davis and V. Bulmus, *Biomacromolecules*, 2008, **9**, 3106–3113.
34 S. Perrier and P. Takolpuckdee, *J. Polym. Sci., Part A: Polym. Chem.*, 2005, **43**, 5347–5393.
35 A. Favier and M. T. Charreyre, *Macromol. Rapid Commun.*, 2006, **27**, 653–692.
36 V. T. Huynh, P. de Souza and M. H. Stenzel, *Macromolecules*, 2011, **44**, 7888–7900.
37 A. Gregory and M. H. Stenzel, *Expert Opin. Drug Delivery*, 2011, **8**, 237–269.
38 K. Gunasekaran, T. H. Nguyen, H. D. Maynard, T. P. Davis and V. Bulmus, *Macromol. Rapid Commun.*, 2011, **32**, 654–659.
39 C. Boyer, P. Priyanto, T. P. Davis, D. Pissuwan, V. Bulmus, M. Kavallaris, W. Y. Teoh, R. Amal, M. Carroll, R. Woodward and T. St Pierre, *J. Mater. Chem.*, 2010, **20**, 255–265.
40 D. Valade, C. Boyer, T. P. Davis and V. Bulmus, *Aust. J. Chem.*, 2009, **62**, 1344–1350.
41 J. Xu, C. Boyer, V. Bulmus and T. P. Davis, *J. Polym. Sci., Part A: Polym. Chem.*, 2009, **47**, 4302–4313.
42 K. L. Heredia, T. H. Nguyen, C.-W. Chang, V. Bulmus, T. P. Davis and H. D. Maynard, *Chem. Commun.*, 2008, 3245–3247.
43 D. Smith, A. C. Holley and C. L. McCormick, *Polym. Chem.*, 2011, **2**, 1428–1441.
44 S. Kirkland-York, Y. Zhang, A. E. Smith, A. W. York, F. Huang and C. L. McCormick, *Biomacromolecules*, 2010, **11**, 1052–1059.
45 A. W. York, F. Huang and C. L. McCormick, *Biomacromolecules*, 2010, **11**, 505–514.
46 A. W. York, Y. L. Zhang, A. C. Holley, Y. L. Guo, F. Q. Huang and C. L. McCormick, *Biomacromolecules*, 2009, **10**, 936–943.
47 D. Pissuwan, C. Boyer, K. Gunasekaran, T. P. Davis and V. Bulmus, *Biomacromolecules*, 2010, **11**, 412–420.
48 C. W. Chang, E. Bays, L. Tao, S. N. S. Alconcel and H. D. Maynard, *Chem. Commun.*, 2009, 3580–3582.
49 Y. Mitsukami, M. S. Donovan, A. B. Lowe and C. L. McCormick, *Macromolecules*, 2001, **34**, 2248–2256.
50 S. H. Thang, Y. K. Chong, R. T. A. Mayadunne, G. Moad and E. Rizzardo, *Tetrahedron Lett.*, 1999, **40**, 2435–2438.
51 P. A. Sivakumar and K. P. Rao, *Biomed. Microdevices*, 2002, **4**, 197–204.
52 Y. X. Zhou and R. M. Kas, *J. Polym. Sci., Part A: Polym. Chem.*, 2008, **46**, 6801–6809.
53 A. C. Devisser, K. Degroot, J. Feyen and A. Bantjes, *J. Polym. Sci., Part C: Polym. Lett.*, 1972, **10**, 851–854.
54 J. M. Benns, J.-S. Choi, R. I. Mahato, J.-S. Park and S. W. Kim, *Bioconjugate Chem.*, 2000, **11**, 637–645.
55 J. M. Benns, R. I. Mahato and S. W. Kim, *J. Controlled Release*, 2002, **79**, 255–269.
56 G. H. Chen and A. S. Hoffman, *Macromol. Chem. Phys.*, 1995, **196**, 1251–1259.
57 M. L. Coote, T. P. Davis, B. Klumperman and M. J. Monteiro, *J. Macromol. Sci., Part C*, 1998, **38**, 567–593.
58 I. SideridouKarayannidou and G. Seretoudi, *Polymer*, 1997, **38**, 4223–4228.
59 W. F. D. Bennett, J. L. MacCallum and D. P. Tieleman, *J. Am. Chem. Soc.*, 2009, **131**, 1972–1978.
60 L. J. Wong, C. Boyer, Z. F. Jia, H. M. Zareie, T. P. Davis and V. Bulmus, *Biomacromolecules*, 2008, **9**, 1934–1944.
61 T. R. Darling, T. P. Davis, M. Fryd, A. A. Gridnev, D. M. Haddleton, S. D. Ittel, R. R. Matheson, G. Moad and E. Rizzardo, *J. Polym. Sci., Part A: Polym. Chem.*, 2000, **38**, 1706–1708.
62 Z. X. Gu, Y. Yuan, J. L. He, M. Z. Zhang and P. H. Ni, *Langmuir*, 2009, **25**, 5199–5208.
63 S. Paasch and E. Brunner, *Anal. Bioanal. Chem.*, 2010, **398**, 2351–2362.
64 L. V. Christensen, C. W. Chang, W. J. Kim, S. W. Kim, Z. Y. Zhong, C. Lin, J. F. J. Engbersen and J. Feijen, *Bioconjugate Chem.*, 2006, **17**, 1233–1240.
65 L. Bromberg, M. Temchenko and T. A. Hatton, *Langmuir*, 2003, **19**, 8675–8684.
66 P. Van de Wetering, N. J. Zuidam, M. J. Van Steenbergen, O. A. G. J. Van der Houwen, W. J. M. Underberg and W. E. Hennink, *Macromolecules*, 1998, **31**, 8063–8068.
67 M. Zhu, L. Xiong, T. Wang, X. Liu, C. Wang and Z. Tong, *React. Funct. Polym.*, 2010, **70**, 267–271.
68 M. A. Ward and T. K. Georgiou, *J. Polym. Sci., Part A: Polym. Chem.*, 2010, **48**, 775–783.
69 D. Fischer, A. von Harpe, K. Kunath, H. Petersen, Y. X. Li and T. Kissel, *Bioconjugate Chem.*, 2002, **13**, 1124–1133.
70 A. K. Varkouhi, M. Scholte, G. Storm and H. J. Haisma, *J. Controlled Release*, 2011, **151**, 220–228.
71 T. Tokatlian and T. Segura, *Wiley Interdiscip. Rev.: Nanomed. Nanobiotechnol.*, 2010, **2**, 305–315.
72 V. Bulmus, *Aust. J. Chem.*, 2005, **58**, 411–422.
73 H. Park, H.-S. Jin, S. Yang and J.-D. Kim, *Colloid Polym. Sci.*, 2009, **287**, 919–926.
74 L. Ma, R. Liu, J. Tan, D. Wang, X. Jin, H. Kang, M. Wu and Y. Huang, *Langmuir*, 2010, **26**, 8697–8703.
75 T. Y. Jiang, Z. Y. Wang, L. X. Tang, F. K. Mo and C. Chen, *J. Appl. Polym. Sci.*, 2006, **99**, 2702–2709.

76 J.-O. You and D. T. Auguste, *Biomaterials*, 2008, **29**, 1950–1957.
77 C. Clawson, L. Ton, S. Aryal, V. Fu, S. Esener and L. Zhang, *Langmuir*, 2011, **27**, 10556–10561.
78 S. Al-Nasiry, N. Geusens, M. Hanssens, C. Luyten and R. Pijnenborg, *Hum. Reprod.*, 2007, **22**, 1304–1309.
79 H. Gloeckner, T. Jonuleit and H.-D. Lemke, *J. Immunol. Methods*, 2001, **252**, 131–138.
80 M. L. Patil, M. Zhang and T. Minko, *ACS Nano*, 2011, **5**, 1877–1887.
81 H. A. Christy, *Adv. Drug Delivery Rev.*, 2006, **58**, 1523–1531.
82 H. de Martimprey, C. Vauthier, C. Malvy and P. Couvreur, *Eur. J. Pharm. Biopharm.*, 2009, **71**, 490–504.
83 H. R. Kim, I. K. Kim, K. H. Bae, S. H. Lee, Y. Lee and T. G. Park, *Mol. Pharmaceutics*, 2008, **5**, 622–631.
84 E. Bertrand, C. Goncalves, L. Billiet, J. P. Gomez, C. Pichon, H. Cheradame, P. Midoux and P. Guegan, *Chem. Commun.*, 2011, **47**, 12547–12549.